Available online at www.sciencedirect.com
ScienceDirect
Polymer 48 (2007) 3413–3419
polymer
www.elsevier.com/locate/polymer

Synthesis of a functionalized polythiophene as an active substrate for a label-free electrochemical genosensor

Hui Peng, Lijuan Zhang, John Spires, Christian Soeller, Jadranka Travas-Sejdic*

Polymer Electronics Research Centre, The University of Auckland, Private Bag 92019, Auckland 1001, New Zealand

Received 18 December 2006; received in revised form 23 March 2007; accepted 11 April 2007
Available online 21 April 2007

Abstract

The synthesis of a new functionalized terthiophene monomer with an unsaturated side chain, 3-((2′:2″,5″:2‴-terthiophene)-3″-yl) acrylic acid, is described. A conducting polymer was obtained by electropolymerization of the functionalized monomer. The properties of the polymer were investigated using FT-IR, Raman and UV–vis spectroscopy. The application of the polymer as an active substrate for a genosensor is demonstrated by the covalent attachment of amino-end modified oligonucleotide probes to the carboxylic acid group of the polymer. The hybridization of the complementary ODNs can be clearly detected by an increase in the admittance without the need for an indicator or any sample modifications.

Keywords: Conducting polymers; Electropolymerisation; DNA sensor

1. Introduction

Detection and quantification of specific DNA sequences are of great importance in numerous applications, such as medical research and clinical diagnosis. Electrochemical genosensors have recently attracted increasing attention because of their simplicity, high selectivity and sensitivity. A variety of schemes, such as metal complexes [1,2], organic redox indicators [3,4], enzymes [5] and nanoparticles [6–8] have been used for the electrochemical detection of DNA hybridization. Besides indirect schemes of this sort, simple and direct electrochemical detection of DNA hybridization [9–13] is of particular interest.

Intrinsically conducting polymers (ICPs) are a relatively new class of polymeric materials that possess a delocalized electronic structure which is sensitive to changes in the polymeric chain environment and other perturbations to the chain conformation. Therefore, grafting of oligonucleotide (ODN) probes onto ICPs would be expected to provide a simple and direct way to detect hybridization events, which perturb the electrochemical response of the polymer. For ICPs to be used as solid substrates for genosensors, the immobilization of oligonucleotide probes can be achieved simply by electrostatic trapping of ODN probes within a growing polymer film [8,14]. However, this approach is not very efficient as steric hindrance complicates the access of the DNA target from the solution to the ODN probes within the film. An alternative approach is covalent immobilization [12,15–18]. Research into the covalent attachment of a biomolecule to amine- or carboxy-functionalized polymers was pioneered by Schuhmann et al. [19]. Garnier and coworkers later proposed a process of functionalization of polypyrrole (PPy) which involves preparation of a precursor polymer film bearing a leaving group, such as an activated ester, at its 3-position, that can be substituted by a 5′-aminoalkyl-terminated ODN probe [20,21]. Cyclic voltammetry experiments after hybridization revealed that the oxidation peak of the polymer shifted in the positive direction and decreased in intensity. Using similar copolymers, Lassalle et al. [22] used changes in the photocurrent spectrum of polypyrrole following hybridization to detect specific DNA sequences.

* Corresponding author.
E-mail address: j.travas-sejdic@auckland.ac.nz (J. Travas-Sejdic).

0032-3861/$ - see front matter © 2007 Elsevier Ltd. All rights reserved.
doi:10.1016/j.polymer.2007.04.029

Numerous functionalized thiophenes have been synthesized in the past due to their favorable properties [23–25]. Generally, most thiophenes with functional groups suitable for immobilization of biomolecules (such as $-NH_2$ and $-COOH$) have been difficult to electropolymerise, because such functional groups exhibit substantial nucleophilicity and attack the radical cation intermediates formed during electropolymerisation, hence inhibiting the polymerization process [26]. While Albery et al. reported the electropolymerisation of thiophene-3-acetic acid in 1991 [27], a high oxidation potential ($\sim$1.6 V vs Ag/Ag^+) and high monomer concentration were necessary to obtain a conducting polymer. At low monomer concentrations, on the other hand, the electrooxidative homopolymerization of thiophene-3-acetate is inhibited [28]. This problem can be avoided using post-polymerization functionalisation since thiophene monomers with protected carboxyl acid group can be easily electropolymerized. This approach is a widely used method for the preparation of new electroactive organic systems with tunable electronic, electrochemical and spectroscopic properties [29,30]. For example, Li et al. synthesized thiophene bearing an activated ester group, *N*-succinimido thiophene-3-acetate, and obtained its homopolymer [31]. A disavantage of the post-polymerization functionalisation process is a potentially detrimental effect on the adherence of the polymer films to the electrode surface, which is of particular importance for electrochemical biosensing. As an alternative route, copolymerisation of functionalized monomers with the corresponding unsubstituted heterocycles was developed based on a copolymer of 3-(oxyalkyl)-thiophene bearing an arylsulfonamide group with 3-methylthiophene used to immobilize amino-end modified DNA probes [32]. Nevertheless, this approach has the disadvantage of not having well defined binding sites on the obtained film.

In this work, we report the synthesis of a new functionalized terthiophene with an unsaturated side chain, 3-((2′:2″,5″:2‴-terthiophene)-3″-yl) acrylic acid (TAA). The monomer can be directly electropolymerised to produce a homopolymer (PTAA) with well defined binding sites. The obtained polymer was characterized by IR, Raman and UV–vis spectroscopy and applied to the development of a genosensor.

2. Experimental

2.1. Materials

Thiophene-3-carboxaldehyde, tetrakis(triphenylphosphine)-palladium [$Pd(PPh_3)_4$], 2-thiophene boronic acid, (triphenylphosphoranylidene) methyl acetate (TPPMA, 98%), 1-ethyl-3-(3-dimethylaminopropyl)carbodiimide (EDC), tetrabutylammonium trifluoromethanesulfonate (TBAFMS) and phosphate buffered saline pellets (PBS, pH 7.4) were obtained from Aldrich. Invitrogen Life Technologies Company synthesized ODNs including probe NH_2-GAT GAG TAT TGA TGC CGA-3′, complementary target 5′-TCG GCA TCA ATA CTC ATC-3′ and noncomplementary 5′-TAT GCT GGT GCG TCG CAC-3′. All aqueous solutions were prepared using Milli-Q water (18.2 MΩ cm). Other chemicals used in this study were of reagent grade or better and were purchased from local commercial sources. All reagents were used as supplied without further purification, unless otherwise stated.

2.2. Monomer synthesis

2.2.1. 3′-Formyl-2:2′,5′:2″-terthiophene (*1*)

3′-Formyl-2:2′,5′:2″-terthiophene was synthesized according to Ref. [23]. ^{1}H NMR (400 MHz, $CDCl_3$, δ/ppm) 10.08 (s, 1H, CHO), 7.56 (s, 1H, H 4′), 7.50 (dd, 1H, H 5), 7.32 (dd, 1H, H 3), 7.30 (dd, 1H, H 5″), 7.23 (dd, 1H, H 3″), 7.16 (dd, 1H, H 4), 7.05 (dd, 1H, H 4″); ^{13}C NMR (400 MHz, $CDCl_3$, δ/ppm) 185.5, 146.3, 138.1, 137.2, 135.9, 132.5, 129.6, 129.0, 128.7, 128.4, 126.2, 125.3, 122.8.

2.2.2. 3-((2′:2″,5″:2‴-Terthiophene)-3″-yl) acrylic acid methyl ester (*2*)

(Triphenylphosphoranylidene) methyl acetate (7.6 mmol, 4 g, 1.5 equiv) was added to a solution of (**1**) (2.1 g, 7.6 mmol) in anhydrous THF (250 mL). The reaction mixture was stirred at 50 °C for 6 h and concentrated in vacuo to give a bright yellow solid, which upon purification by column chromatography on silica gel (hexane/ethyl acetate = 5:1) gave the product (**2**) (2.1 g, 83%). ^{1}H NMR ($CDCl_3$, δ/ppm), 7.90 (d, 1H, C*H*=CHCOOCH$_3$), 7.42 (dd, 1H, H 5′), 7.32 (s, 1H, H 4″), 7.27 (dd, 1H, H 3′), 7.20 (dd, 1H, H 5‴), 7.18 (dd, 1H, H 3‴), 7.14 (dd, 1H, H 4′), 7.04 (dd, 1H, H 4‴), 6.36 (d, 1H, CH=C*H*COOCH$_3$); 3.79 (s, 3H); ^{13}C NMR (400 MHz, $CDCl_3$, δ/ppm) 167.92, 137.57, 137.25, 137.09, 136.43, 134.18, 134.02, 128.78, 128.46, 128.34, 127.82, 125.66, 124.88, 122.34; 119.26, 52.07.

2.2.3. 3-((2′:2″,5″:2‴-Terthiophene)-3″-yl) acrylic acid (TAA) (*3*)

Compound **2** (1 g, 3 mmol) was placed in 30 mL of 1:1 (v:v) mixture of MeOH and 2 M aqueous NaOH and refluxed for 5 h, after which time the reaction mixture was allowed to cool and methanol was removed by vacuum. The aqueous solution was acidified with 5 M HCl to pH 3 and the precipitate was collected and dried in a vacuum oven to give a yellow powder of (**3**) (0.84 g, 88%). IR (KBr, cm^{-1}) 3450, 3000, 1678, 1612, 1422, 1288, 1206, 970, 844, 702; ^{1}H NMR ($CDCl_3$, δ/ppm), 7.99 (d, 1H, C*H*=CHCOOH), 7.44 (dd, 1H, H 5′), 7.35 (s, 1H, H 4″), 7.29 (dd, 1H, H 3′), 7.22 (dd, 1H, H 5‴), 7.20 (dd, 1H, H 3‴), 7.14 (dd, 1H, H 4′), 7.06 (dd, 1H, H 4‴), 6.37 (d, 1H, CH=C*H*COOH); ^{13}C NMR (400 MHz, $CDCl_3$, δ/ppm) 170.85, 139.26, 138.44, 137.29, 136.34, 134.05, 133.78, 128.55, 128.48, 128.38, 128.04, 125.80, 125.00; 122.31, 118.22. MS (m + 1): 319.3.

2.3. Electropolymerization

The electropolymerization was carried out by cyclic voltammetry from 0 to +1.3 V at a scan rate of 100 mV/s using a CH Instrument electrochemical workstation (Model 440, CH Instruments, USA). A three-electrode cell with a volume of 10.0 mL, comprising a Pt (BAS, 1.0 mm diameter) or a glassy carbon

(BAS, 3.0 mm diameter, 7.07 mm^2 geometrical area) working electrode, an Ag/AgCl (3 M KCl) reference electrode and a Pt wire counter electrode. Prior to electropolymerisation, the working electrode was polished with 0.5 μm alumina slurry, then sonicated in acetonitrile containing active carbon powder, chloroform and Milli-Q water for 10 min. The polymerization solution contained 0.05 M TBAFMS and 0.005 M 3-((2′:2″, 5″:2‴-terthiophene)-3″-yl) acrylic acid (TAA) in dichloromethane. For the UV–vis and scanning electron microscopy experiments, the polymer was electrochemically deposited on an indium tin oxide (ITO)-coated glass electrode.

2.4. FT-IR and Raman spectroscopy

The PTAA and polythiophene samples for FT-IR spectroscopy were prepared by using stainless steel working electrodes at a fixed potential of +1.3 V and +1.2 V, respectively. After washing with acetone and drying in a vacuum oven, the polymer samples were prepared with KBr and formed into discs for FT-IR spectral analysis. The spectra were recorded using a Bio-Rad FT-IR spectrometer, model FTS-60.

For *in situ* Raman spectroscopy measurement PTAA was deposited onto the surface of a Pt electrode by cyclic voltammetry from 0 to +1.3 V at a scan rate of 100 mV/s. The spectra were recorded at different applied potentials using a Renishaw Raman spectrometer (system 1000) with 785 nm (red) laser excitation.

2.5. Immobilization of ODN probe and hybridization

The grafting of ODN probes onto the PTAA film was performed according to a previously described procedure [12,33]. To covalently attach the ODN probe 40 μL of phosphate buffer (pH 5.2) containing 20 nmol ODN probe and 400 nmol EDC was applied to the surface of a PTAA-coated electrode, and kept at 28 °C for 1 h. Finally, the modified electrode was thoroughly washed using PBS solution (pH 7.4) in order to remove any remaining unattached ODN probes.

Hybridization was carried out by incubating the ODN probe-modified films in PBS solution (pH 7.4) containing ODN samples for 1 h at 42.0 °C. After hybridization, the electrode was washed three times using PBS solution to remove any non-hybridized ODNs.

2.6. Electrochemical impedance measurement

Electrochemical impedance spectra were recorded in PBS solution (pH 7.4) before and after hybridization using an EG&G potentiostat/galvanostat (model 280, Princeton Applied Research) coupled to an EG&G 1025 Frequency Response Analyzer. A conventional three-electrode cell containing a modified glassy carbon working electrode, Pt slide counter electrode and Ag/AgCl (in 3 M KCl) reference electrode was used. The impedance experiments were run with 10 mV sinusoidal excitation amplitude at an applied bias potential of 800 mV. The impedance data were measured and collected at harmonic frequencies from 1 Hz to 1 MHz.

3. Results and discussion

3.1. Electropolymerization and characterization

The synthesis scheme for TAA is shown in Scheme 1. A Wittig condensation between 3′-formyl-2:2′,5′:2″-terthiophene (**1**) and TPPMA proceeded to 3-((2′:2″,5″:2‴-terthiophene)-3″-yl) acrylic acid methyl ester (**2**), which was hydrolyzed to obtain the desired monomer (**3**). The monomer TAA is a trans-isomer as deduced from its ^1H NMR spectrum, which is in accordance with previous reports in the literature [34,35]. Fig. 1 shows the UV–vis spectrum of TAA. There are two well-resolved absorption peaks at 336 and 287 nm. Comparing the TAA spectrum with the UV–vis spectrum of terthiophene [36,37], the peak at 336 nm can be ascribed to thienyl chromophores and the peak at 287 nm to the presence of the conjugated side chain.

A typical polymerization voltammogram is presented in Fig. 2A. TAA is electropolymerized at potentials higher than +1.1 V vs Ag/AgCl. The first cycle (Fig. 2A, inset) shows the ''nucleation loop'' where the scan is reversed on the rising part of the peak, which is typical for a voltammogram of monomers yielding conducting polymers [38]. During continuous potential scanning, the oxidation current at around +1.3 V progressively increased which further confirms that an electroactive polymer was deposited onto the electrode surface. The color of the polymer changed from brown to dark blue with increasing film thickness. Unlike alkyl substituted polythiophene [30], the obtained polymer was not soluble in common organic solvents such as acetonitrile, dichloromethane and propylene carbonate. Fig. 2B presents the cyclic voltammogram of a PTAA film in a monomer free solution. An anodic peak at +0.64 V appears as a broad shoulder preceding a second broad peak at +1.0 V. The corresponding cathodic peaks are located at +0.82 V and +0.46 V. The presence of two anodic peaks is usually attributed to either polaron and subsequent bipolaron formation [39], or to the coexistence

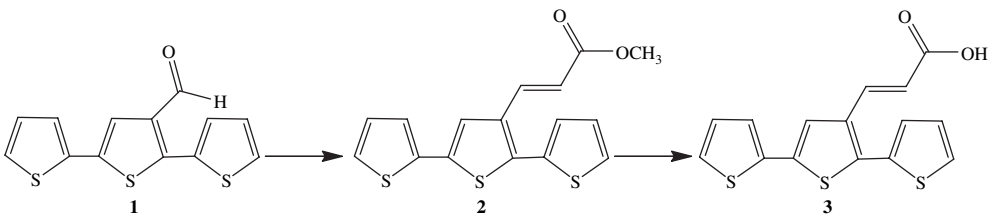

Scheme 1. Synthesis route of TAA.

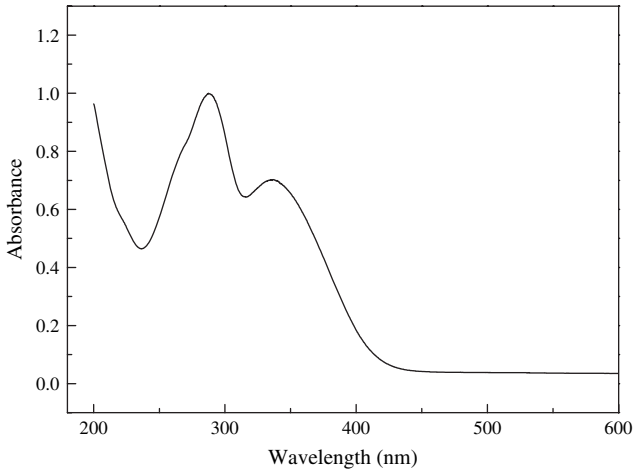

Fig. 1. UV–vis spectrum of TAA in CH_2Cl_2.

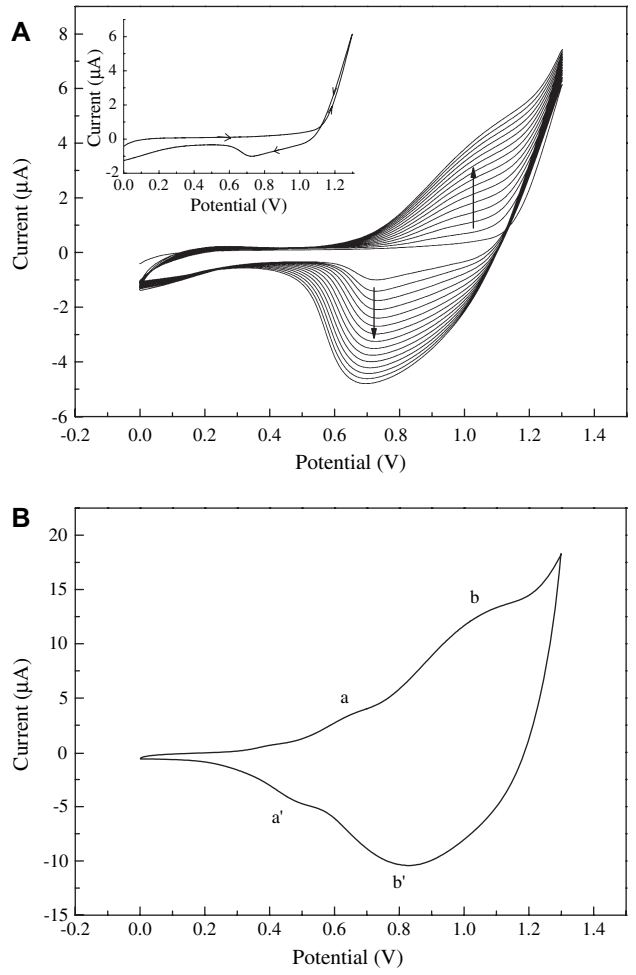

Fig. 2. (A) Electrochemical growth of PTAA on a platinum electrode using cyclic voltammetry at a scan rate of 100 mV/s. Fifteen cycles were taken between 0 V and 1.3 V. Inset: the first CV cycle. (B) Cyclic voltammogram of a PTAA film in 0.1 M TBAFMS of dichloromethane solution at a scan rate of 50 mV/s.

of two distinct distributions of macromolecular weights within the polymer film with different conjugation lengths [40]. A strong increase in the anodic current can be seen at potentials greater than +1.2 V, indicating the beginning of polymer overoxidation.

A PTAA film was further investigated by UV–vis spectroelectrochemistry. A polymer film was deposited onto an ITO electrode and UV–vis spectra were measured *in situ* as different potentials were applied. The results are presented in Fig. 3. When the applied potential was lower than +0.4 V, there was no obvious change in the recorded spectra. According to the cyclic voltammogram (Fig. 2B), PTAA is in the neutral state at these potentials. A strong absorption band at 487 nm is attributed to a $\pi \rightarrow \pi^*$ transition in the conjugated polymer backbone. The spectrum begins to change at +0.5 V, i.e. at the potential at which polymer oxidation starts in accordance with observations seen in Fig. 2B. A progressive increase in the applied potential leads to a decrease in the amplitude of the $\pi \rightarrow \pi^*$ transition band at 487 nm and an increase in absorbance at wavelengths higher than 650 nm. At potentials lower than +0.8 V an equilibrium between the neutral and polaronic forms in PTAA is indicated by an isosbestic point at 585 nm. When the applied potentials were above +0.9 V, the spectra showed a new isosbestic point located at 544 nm and a new absorption band appeared at 663 nm. This result indicates a new equilibrium between two different neutral and polaronic forms of the polymer, characterized by shorter conjugation length [41].

A typical FT-IR spectrum of doped PTAA is shown in Fig. 4. For comparative purposes, Fig. 4 also shows a spectrum of polythiophene prepared from a bithiophene monomer. The spectrum of PTAA (Fig. 4, curve a) is quite similar to that of polythiophene (curve b) except for a strong absorption peak at 1678 cm^{-1} characteristic of the stretching vibration of the carbonyl group. CH out-of-plane bending vibrations characteristic of 2,5-substitued thiophene rings appear in the range of 900–600 cm^{-1} with the strongest peaks around 786–790 cm^{-1} [42]. Therefore, the infrared band at 793 cm^{-1} in the spectrum of PTAA, which is shifted by 3 cm^{-1} compared to polythiophene, illustrates that polymerization occurs at the 5′ and 5‴ positions of the terthiophene monomer units.

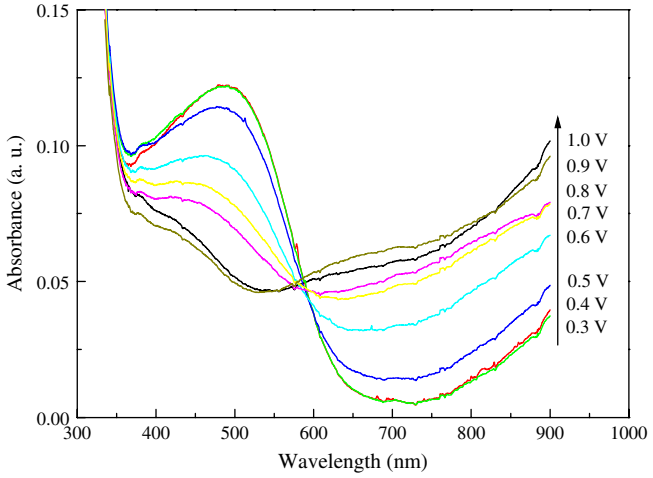

Fig. 3. *In situ* UV–vis spectra of PTAA film deposited on an ITO electrode at different applied potentials.

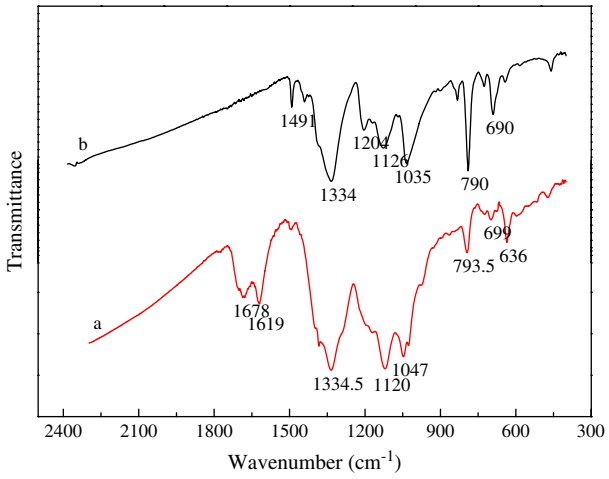

Fig. 4. FT-IR spectra of PTAA (a) and polythiophene (b).

The Raman spectra of doped PTAA and polythiophene films on a stainless steel electrode are shown in Fig. 5 and the assignments of Raman bands are listed in Table 1 with reference to a previous publication [43]. It can be seen that both spectra have similar features. However, due to the existence of conjugated side chains in PTAA, the bands originating from C_α=C_β ring stretching at 1484 cm^{-1} and symmetric stretching of radical cations of PTAA at 1436 cm^{-1} are shifted toward higher wave numbers compared to those of polythiophene. Furthermore, there is a clear shoulder band at 1178 cm^{-1}, between the doublet assigned to C_α–$C_{\alpha'}$ stretching (1223 and 1155 cm^{-1}), which we attribute to the presence of the conjugated side chain.

The doping process of PTAA was also investigated by *in situ* measurement of Raman spectra with a PTAA modified Pt electrode at various potentials. Fig. 6 shows the collected Raman spectra with increasing electrode potentials. From the cyclic voltammogram of PTAA, we know that PTAA is

Table 1
Band assignment of Raman spectra of PTAA and polythiophene

Assignments	PTAA (cm^{-1})	Polythiophene (cm^{-1})
C_α=C_β ring stretching	1484	1478
Quinoid (radical cations)	1436	1428
C_β–$C_{\beta'}$ ring stretching	1352	1351
C_α–$C_{\alpha'}$ stretching	1223	1222
C_α–$C_{\alpha'}$ stretching (anti)	1155	1154
C_β–H bending	1059	1054
Ring deformation C–S–C	734	731
Ring deformation C–S–C	692	691

in the neutral state at a potential less than +0.5 V. Since PTAA is in its neutral state, it is out of resonance with the 785 nm laser excitation, as judged from the UV–vis spectrum (Fig. 3); there is only one weak band at 1462 cm^{-1} in the spectral range where C_α=C_β symmetric or antisymmetric stretching vibrations are expected [43] (note: the band at 923 cm^{-1} is due to the TBAFMS–acetonitrile solution. See also the Raman spectrum of the bare Pt electrode in a TBAFMS–acetonitrile solution in Fig. 6). As the electrode potential was increased, the intensities of the vibration bands of the polymer increased. When the electrode potential reached +0.7 V, a Raman spectrum containing the characteristic bands of doped PTAA was obtained. This is consistent with the cyclic voltammogram of PTAA which shows that the oxidized polymer is starting to form at this potential. The band of C_α=C_β stretching deformation in oxidized PTAA is red shifted to 1436 cm^{-1} compared to the corresponding band for the neutral polymer due to the doping induced force constant weakening [44]. The intensity of this band increased at a higher doping level caused by an increase in the electrode potential. The bands in the spectral range of 1150–1230 cm^{-1} are assigned to C_α–$C_{\alpha'}$ stretching and C_β–H bending. The bands originating from the C–S deformation in the thiophene ring appeared in the range of 680–750 cm^{-1}, which became more pronounced

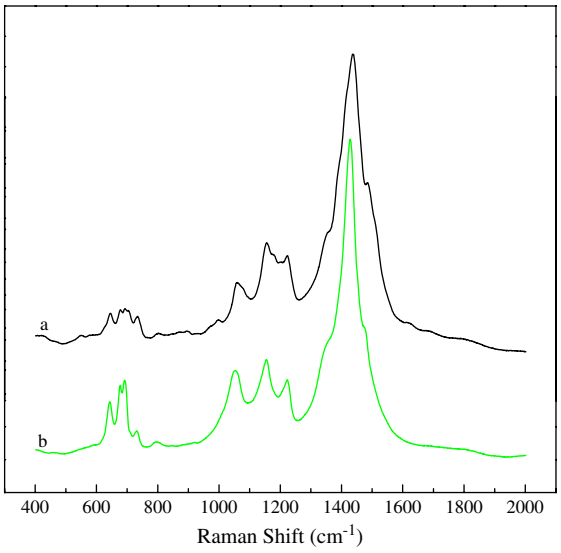

Fig. 5. Raman spectra of doped PTAA (a) and doped polythiophene (b) deposited on a stainless steel electrode under 718 nm laser excitation.

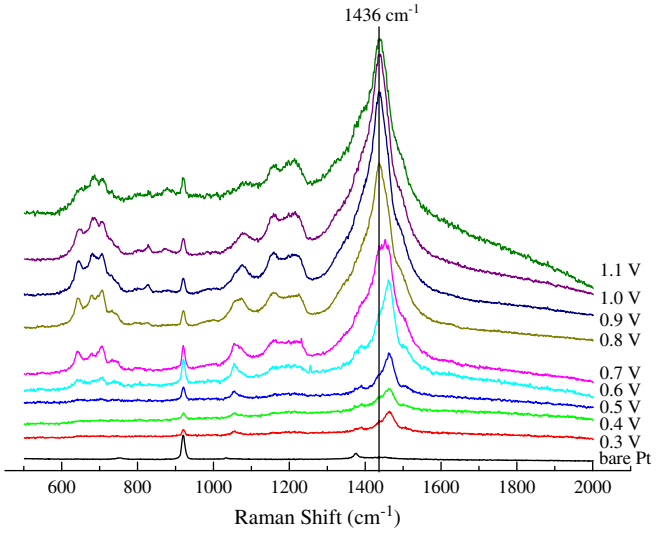

Fig. 6. *In situ* Raman spectra of PTAA deposited on a Pt electrode recorded at different electrode potentials in 0.1 M TBAFMS in acetonitrile solution. λ_{exc} = 718 nm.

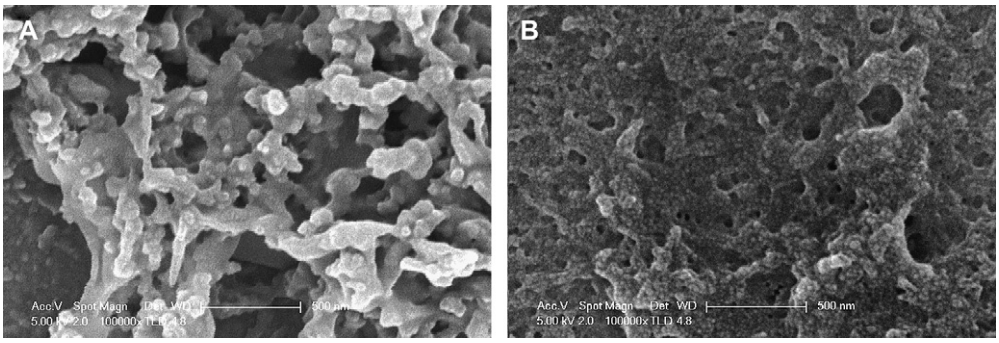

Fig. 7. SEM images of polythiophene (A) and PTAA (B).

upon doping. When the potential reached +1.1 V, the Raman bands started to broaden and the intensities decrease, pointing to oxidative degradation of the polymer which usually follows oxidative doping at higher potentials.

The morphology of the obtained polymer films is dependent on the kinetics of nucleation and growth of the polymer, which, in turn, generally depends on the structure of the monomer, the nature of the dopant, and the polymerization conditions. SEM images showed that PTAA and polythiophene films prepared under similar conditions had quite different morphologies (Fig. 7). The polythiophene film was porous and had a fibre-like structure, while the PTAA film exhibited a much denser morphology. This may be due to an increase in polarity of the monomer caused by the carboxylic acid substituent.

3.2. Detection of hybridization

For the detection of DNA hybridization, a thin PTAA film was prepared by cyclic voltammetry as described in the experimental section. The amino-end modified ODN probes were grafted onto the PTAA film by formation of covalent bonds between carboxylic acid and amino groups catalyzed by EDC. Electrochemical impedance measurements were performed on the ODN probes-modified PTAA film in PBS buffer before and after incubation with complementary or noncomplementary ODN solutions. The results are shown in Fig. 8 in the form of admittance spectra. After incubation with complementary ODN solution, a significant increase in the admittance was observed (Fig. 8A), indicating that the formation of ODN duplexes caused a change in the conducting properties of the sensing polymer layer. By contrast, the admittance spectra exhibited little change after incubation with noncomplementary ODN solution (Fig. 8B). A possible reason for the increased conductance are changes in ODN conformation following hybridization, where the originally single-stranded ODN behaved as random coils lying flat onto the polymer film surface, while the double-stranded ODN formed a more rigid double helix structure that liberates the surface of the PTAA film and facilitates the ion exchange during the doping process [32].

4. Conclusion

In this study, a new functionalized terthiophene monomer with an unsaturated side chain, 3-((2′:2″,5″:2‴-terthiophene)-3″-yl) acrylic acid was synthesized. Electropolymerisation to a conducting polymer film was straightforward. This methodology overcomes the polymerization difficulties exhibited by carboxylic acid substituted thiophene monomers, as

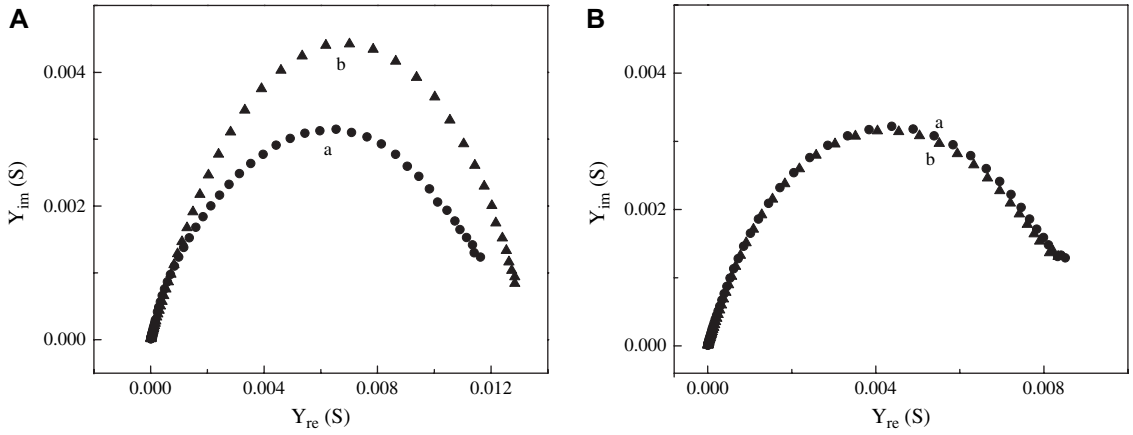

Fig. 8. Admittance spectra. A: (a) PTAA film after immobilization of the probe, (b) after incubation with 4.03 μM complementary ODN; B: (a) PTAA film after immobilization of the probe, (b) after incubation with 4.03 μM noncomplementary ODN.

mentioned above. The obtained polymer was characterized by FT-IR, Raman and UV–vis spectroscopy and use of the polymer for biosensing was demonstrated by covalently grafting an amino-end modified ODN probe to the carboxylic acid group on the polymer. The hybridization of the complementary ODNs could be detected by an increase in the film admittance thus establishing a novel indicator- and label-free electrochemical DNA assay.

Acknowledgement

This work was financially supported by the Royal Society of New Zealand (Marsden Fund).

References

[1] Erdem A, Meric B, Kerman K, Dalbasti T, Ozsoz M. Electroanalysis 1999;11:1372.
[2] Takenaka S, Yamashita K, Takagi M, Uto Y, Kondo H. Anal Chem 2000;72:1334.
[3] Hashimoto K, Ito K, Ishimori Y. Anal Chem 1994;66:3830.
[4] Millan KM, Mikkelsen SR. Anal Chem 1993;65:2317.
[5] Carpini G, Lucarelli F, Marrazza G, Mascini M. Biosens Bioelectron 2004;20:167.
[6] Wang J, Xu D, Kawde A-N, Polsky R. Anal Chem 2001;73:5576.
[7] Wang J, Liu G, Merkoci A. J Am Chem Soc 2003;125:3214.
[8] Peng H, Soeller C, Cannell MB, Bowmaker GA, Cooney RP, Travas-Sejdic J. Biosens Bioelectron 2006;21:1727.
[9] Karadeniz H, Gulmez B, Sahinci F, Erdem A, Kaya GI, Unver N, et al. J Pharm Biomed Anal 2003;33:295.
[10] Singhal P, Kuhr WG. Anal Chem 1997;69:4828.
[11] Kerman K, Morita Y, Takamura Y, Tamiya E. Electrochem Commun 2003;5:887.
[12] Peng H, Soeller C, Vigar N, Kilmartin Paul A, Cannell Mark B, Bowmaker Graham A, et al. Biosens Bioelectron 2005;20:1821.
[13] Wang J, Rivas G, Fernandes JR, Lopez Paz JL, Jiang M, Waymire R. Anal Chim Acta 1998;375:197.
[14] Komarova E, Aldissi M, Bogomolova A. Biosens Bioelectron 2005; 21:182.
[15] Godillot P, Korri-Youssoufi H, Srivastava P, El Kassmi A, Garnier F. Synth Met 1996;83:117.
[16] Livache T, Roget A, Dejean E, Barthet C, Bidan G, Teoule R. Nucleic Acids Res 1994;22:2915.
[17] Lassalle N, Roget A, Livache T, Mailley P, Vieil E. Talanta 2001;55:993.
[18] Peng H, Soeller C, Travas-Sejdic J. Macromolecules 2007;40:909.
[19] Schuhmann W, Lammert R, Uhe B, Schmidt HL. Sens Actuators B-Chem 1990;B1:537.
[20] Korri-Youssoufi H, Yassar A. Biomacromolecules 2001;2:58.
[21] Korri-Youssoufi H, Garnier F, Srivastava P, Godillot P, Yassar A. J Am Chem Soc 1997;119:7388.
[22] Lassalle N, Mailley P, Vieil E, Livache T, Roget A, Correia JP, et al. J Electroanal Chem 2001;509:48.
[23] Collis GE, Burrell AK, Scott SM, Officer DL. J Org Chem 2003;68:8974.
[24] Guernion NJL, Hayes W. Curr Org Chem 2004;8:637.
[25] Demadrille R, Divisia-Blohorn B, Zagorska M, Quillard S, Rannou P, Travers JP, et al. New J Chem 2003;27:1479.
[26] Li G, Kossmehl G, Welzel H-P, Engelmann G, Hunnius W-D, Plieth W, et al. Macromol Chem Phys 1998;199:525.
[27] Albery WJ, Li F, Mount AR. J Electroanal Chem Interf Electrochem 1991;310:239.
[28] Welzel H-P, Kossmehl G, Stein H-J, Schneider J, Plieth W. Electrochim Acta 1995;40:577.
[29] McCullough RD. Adv Mater 1998;10:93.
[30] Buga K, Pokrop R, Majkowska A, Zagorska M, Planes J, Genoud F, et al. J Mater Chem 2006;16:2150.
[31] Li G, Kossmehl G, Welzel H-P, Engelmann G, Hunnius W-D, Plieth W, et al. Macromol Chem Phys 1998;199:2255.
[32] Gautier C, Cougnon C, Pilard J-F, Casse N. J Electroanal Chem 2006;587:276.
[33] Walsh MK, Wang X, Weimer BC. J Biochem Biophys Methods 2001; 47:221.
[34] Zhou E, He C, Tan Za, Yang C, Li Y. J Polym Sci Polym Chem 2006;44:4916.
[35] Zhou E, Hou J, Yang C, Li Y. J Polym Sci Polym Chem 2006;44: 2206.
[36] Kankare J, Lukkari J, Pasanen P, Sillanpaa R, Laine H, Harmaa K, et al. Macromolecules 1994;27:4327.
[37] Wagner P, Officer DL. Synth Met 2005;154:325.
[38] Downard AJ, Pletcher D. J Electroanal Chem Interf Electrochem 1986;206:147.
[39] Chen X, Inganaes O. J Phys Chem 1996;100:15202.
[40] Szkurlat A, Palys B, Mieczkowski J, Skompska M. Electrochim Acta 2003;48:3665.
[41] Zanardi C, Scanu R, Pigani L, Pilo MI, Sanna G, Seeber R, et al. Synth Met 2006;156:984.
[42] Akimoto M, Furukawa Y, Takeuchi H, Harada I, Soma Y, Soma M. Synth Met 1986;15:353.
[43] Bazzaoui EA, Levi G, Aeiyach S, Aubard J, Marsault JP, Lacaze PC. J Phys Chem 1995;99:6628.
[44] Louarn G, Trznadel M, Buisson JP, Laska J, Pron A, Lapkowski M, et al. J Phys Chem 1996;100:12532.